Journal of Petroleum Science and Technology 14(4): 44, 2024, Pages 28-36
DOI:10.22078/jpst.2025.5534.1951

Journal of Petroleum Science and Technology
Research Paper
https://jpst.ripi.ir/

Improving geosteering performance using rate of penetration and gas ratio: case studies in a limestone reservoir

Sina Fathi Hafshejani[1], Mohamadmehdy Ahi[2] and Saeid Jamshidi[1]*

1. Department of Chemical & Petroleum Engineering, Sharif University of Technology, Tehran, Iran

2. Reppco Company, Tehran, Iran

Abstract

Geosteering is an essential method employed in oil and gas drilling, particularly for horizontal wells, to precisely locate the wellbore within hydrocarbon-rich formations. To carry out this process, the gamma-ray logs from the laterals are matched with logs from a reference vertical well to position the lateral in the desired path accurately. Numerous studies have been carried out in the field of geosteering, focusing on the application of machine learning and the creation of automated geosteering methods. Due to the high cost of repeated use of steering, it can be helpful to establish a logical mathematical correlation between two or more parameters for movement within the reservoir. This study investigates the relationship between Rate of Penetration (ROP) and gas ratio data in three laterals drilled in a heterogeneous limestone reservoir in Iran by plotting normalized ROP vs. normalized gas ratio. Geomaster software is used to direct the geosteering process in order to ascertain the reservoir's depth. Once the ROP and gas ratio data have been normalized and outliers removed, different models such as linear, polynomial, power, and exponential are utilized in MATLAB. As a result, we can observe that for the majority of laterals, the second-degree polynomial model offers the best correlation. Also, the presence of heterogeneity affects some results of laterals. These results can be applied to reduce the expenses associated with recurrent geosteering operations, enable the drilling of new or extended laterals, and optimize drilling operations in the field.

Keywords: Gas ratio, Geosteering, Rate of Penetration, Limestone reservoir, Drilling optimization.

Introduction

The method of geosteering involves changing a directional or horizontal wellbore's trajectory to optimize contact with a reservoir's hydrocarbon-bearing zones. There are two main approaches to accomplish this: one model-based and the other strat-based (Fig. 1).

This technique is crucial for optimizing production and reducing the cost of drilling operations. Instruments like Measurement While Drilling (MWD) and Logging While Drilling (LWD) offer real-time information, allowing for modifications to the well's path according to the features of the reservoir.

ROP is the distance drilled per unit of time. Several factors influence it, such as mud weight, weight on bit, and the lithology of the formation [2]. ROP is used to evaluate the properties of the formation and ascertain the target depth. Another critical parameter in this paper is the gas ratio, which may deviate due to changes in lithology or drilling events in the well, such as introducing drilling fluid into the formation, changes in ROP, or variations in bit size.

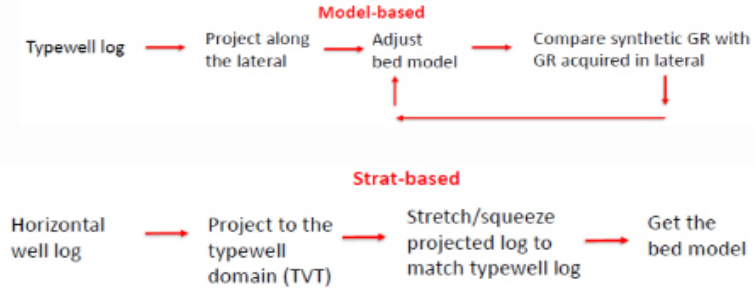

Fig. 1 Model-based and Strat-based procedure, [1].

**Corresponding author:* Saeid Jamshidi, Department of Chemical & Petroleum Engineering, Sharif University of Technology, Tehran, Iran
E-mail addresses: jamshidi@sharif.edu
Received 2024-09-04, Received in revised form 2025-06-30, Accepted 2025-07-13, Available online 2025-11-04

Higher ROP and gas ratio readings are the consequence of porosity and hydrocarbons in reservoir layers. The reservoir and its lithology can be somewhat identified using this relationship. For example, soft formations show high ROP, while shales exhibit a lower gas ratio [3,4].

In recent years, researchers have become interested in improving geosteering, including predicting a log (Fig. 2) based on offset wells and calculating the true stratigraphic thickness (TST) to the drilled point correlated with the LWD log through matching. This work has improved well placement in the reservoir by enhancing the accuracy of subsurface models and their dynamic updating [5].

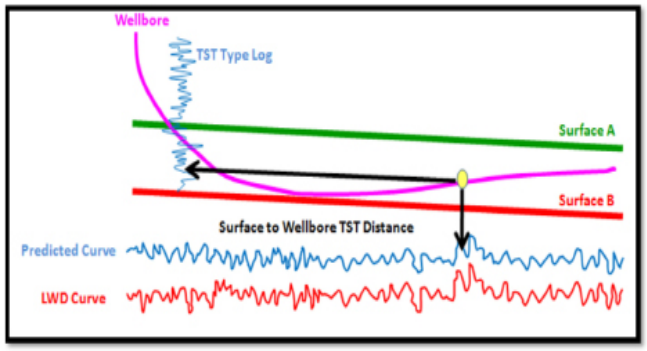

Fig. 2 Well log prediction process, [5].

Creating an automatic geosteering algorithm using a stratigraphic misfit heatmap (Fig. 3) is an innovative approach in geosteering. This algorithm can effectively detect faults and calculate the probability of the well being placed in the desired path. Additionally, it can establish correlations [6]. Control points can be utilized to improve the accuracy of automated geosteering when it produces unreasonable interpretations [7]. Estimating geological boundaries using well-log data can lead to automatic steering [8].

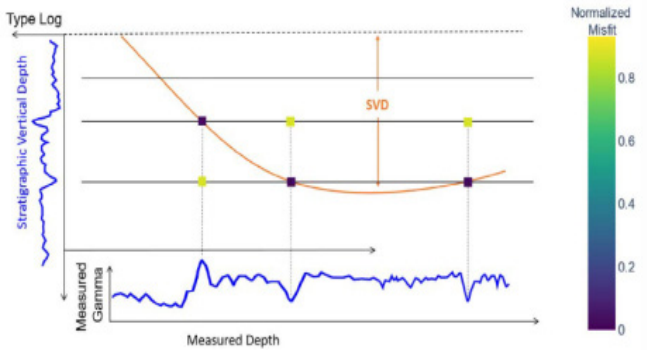

Fig. 3 Lateral and reference well gamma-ray correlation in stratigraphic misfit heatmap, [6].

By employing relevant models, a support system is utilized to enhance geological uncertainties [9] or making appropriate decisions regarding drilling operations [10]. The Bayesian Decision Network is another system used in geosteering that displays the errors of the instruments and geological events [11].

To achieve the goals of geosteering, the Stochastic Monte Carlo method [12] or Bayesian Network [13] can be used to solve inverse geosteering problems. Resistivity tools play an essential role in geosteering, leading to lateral guidance in complex reservoirs and providing subsurface information [14,15].

3D maps have made it possible to create a better view of reservoirs, wells, and geological layering features [16,17]. Drilling costs can be reduced by developing a 3D geosteering system that combines engineering and geology [18] and geological interpretation can be conducted using its features [19].

Logs between lateral and typewell were correlated using machine learning to build an autonomous geosteering model for better well siting in the target path. Finally, the advantages of this method include reducing human errors and increasing operational efficiency through automated steering [20]. Machine learning was also used to predict lithology by correlating drill string and bit data [21] or utilizing LWD data [22].

Although advances in machine learning and automation have significantly improved geosteering accuracy, the high costs associated with this process remain a challenge. For this reason, developing predictive models that correlate drilling parameters such as the ROP and gas ratio with reservoir characteristics can significantly reduce the need for repeated geosteering. Studying three well data in a reservoir and obtaining correlations with different accuracies can help us identify a heterogeneous reservoir and its geomechanical properties, including resistance and stresses on the rock, as well as identify faults, natural fractures, anticlines, etc.

The purpose of this investigation is to developing a correlation between ROP and gas ratio reservoir data from three laterals drilled in a heterogeneous limestone reservoir in Iran. The average WOB in drilling the reservoir layer for laterals 1, 2, and 3 is 12, 9, and 12 kIb, respectively. The goal is to establish predictive models to guide future lateral drilling in the field without requiring costly geosteering processes. We used various mathematical models to assess the accuracy of these correlations and determine the most reliable method for optimizing drilling operations.

Methodology

Field Overview

The field under study is a heterogeneous limestone reservoir located in Iran. Three laterals were drilled and geosteered using Geomaster software to accurately position the wellbores within the hydrocarbon-bearing zones of the reservoir. During the drilling of these laterals, information on the ROP and gas ratio was gathered.

To evaluate initially the reservoir and find the depth of the desired layer, first, we used ROP and gas ratio data in reference (vertical) well like in Fig. 4. In this Figure, we saw approximately that both charts at Measurement depth (MD) =2600 m to MD=2700 m (in vertical well, MD equals True Vertical Depth (TVD)) have increased. So, the reservoir layer may be placed at this depth; however, it should be geosteered for a more accurate assessment.

Geosteering Process

The geosteering procedure for the three laterals was guided by Geomaster software. By analyzing gamma-ray logs, we accurately determined the exact depth and thickness of the reservoir. The gamma-ray logs from the laterals were matched with logs from a reference vertical well to improve the accuracy of the wellbore placement.

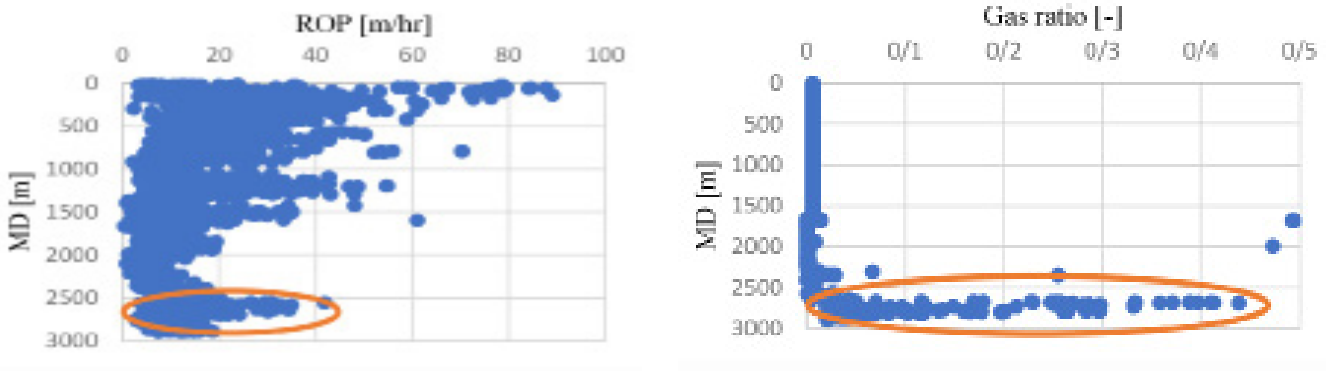

Fig. 4 MD graphs in terms of ROP and gas ratio in reference well of lateral 1.

As seen in Fig.s 5, 6, and 7, this matching method enabled us to adjust the well trajectory in response to the real-time determination of reservoir boundaries. In all the laterals, according to their geosteering, the reservoir layer was located between Sar. 3 and Sar. 4-7, and the green area of this layer indicates the desired portion. Furthermore, in lateral 1, as analyzed in Fig. 4, the reservoir depth is approximately.

Data Normalization and Outlier Removal

Using real data and the presence of heterogeneity create outliers that must be removed. Equation 1 was used to normalize the data between 0 and 1. This normalization eliminated the effects of scale differences between the two datasets.

The first and third quartile methods were then applied to eliminate outliers. This method involved calculating the interquartile range (IQR) and removing data points that fell outside 1.5 times the IQR above the third quartile or below the first quartile (The reservoir data obtained through geosteering has been utilized in this project.).

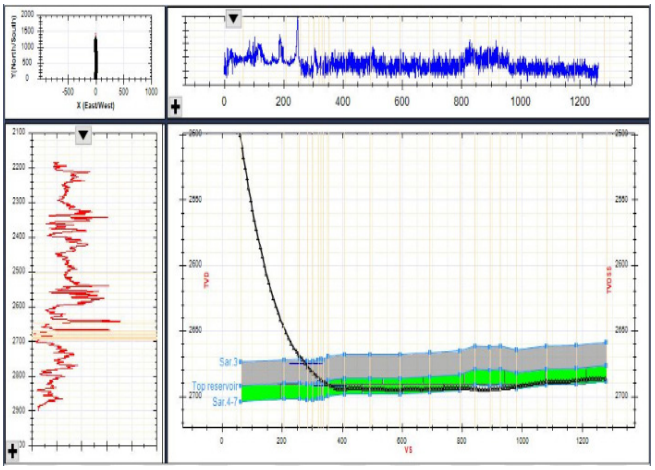

Fig. 5 Geosteering of lateral 1.

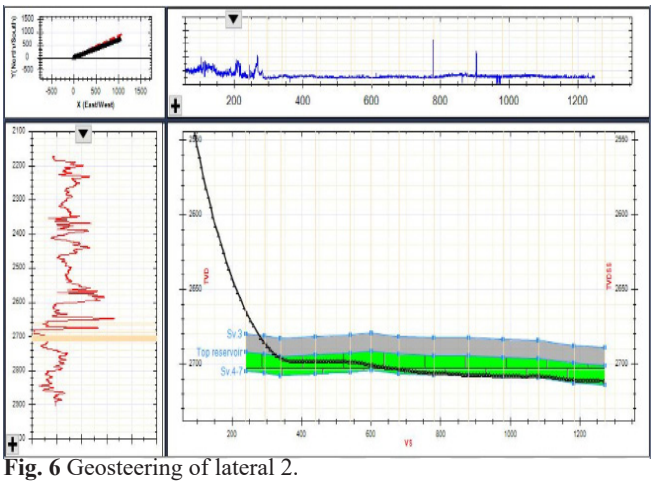

Fig. 6 Geosteering of lateral 2.

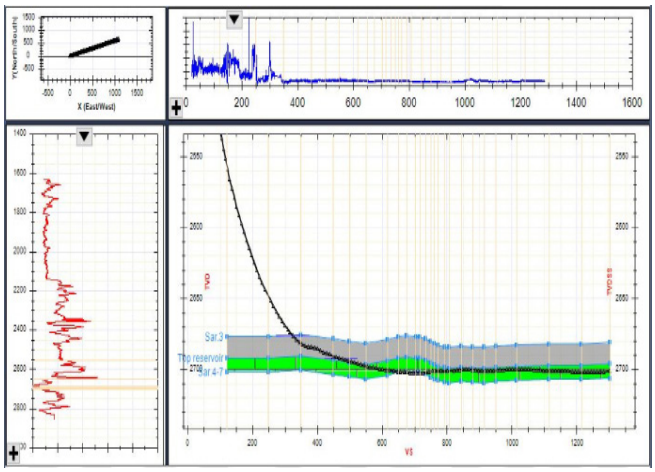

Fig. 7 Geosteering of lateral 3.

$$x_{norm} = \frac{x - x_{\min}}{x_{\min} - x_{\max}} \quad [-] \qquad (1)$$

Gas ratio (@ MD=3080 m): 0.633 [-]
Minimum gas ratio in total data: 0.117
Maximum gas ratio in total data: 42.511

$$gas - ratio_{norm} = \frac{0.633 - 1.117}{42.511 - 1.117} = 0.01217 \qquad (2)$$

ROP (@ MD=3080 m): 10.86 [m/hr]
Minimum ROP in total data: 1.68
Maximum ROP in total data: 29.27

$$ROP_{norm} = \frac{10.86 - 1.68}{29.27 - 1.68} = 0.3327 \qquad (3)$$

The upper and lower limits of the gas ratio and ROP are shown in Table 1:

Table 1 Removing outlier data using the first and third quartile method in Excel-lateral 1

Parameter	Command in Excel	Gas ratio [-]	ROP [m/hr]
First Quarter	QUARTILE.EXC(: ,1) (First Quarter Command)	0.2249	0.15
Third Quarter	QUARTILE.EXC(: ,3) (Third Quarter Command)	0.3455	0.399
50%	Third Quarter-First Quarter	0.1206	0.249
Upper limit	Third Quarter+(1.5*50%)	0.5265	0.772
Lower limit	First Quarter-(1.5*50%)	0.0439	-0.2234

* A negative value indicates no lower limit.

Only data larger than the upper limit were eliminated as outliers because the ROP lower limit is negative. Finally, as an example, a portion of the calculations related to normalizing data and removing outliers for lateral 1 is shown in Table 2 (Red data are outliers):

Table 2 A portion of the information and calculations of lateral 1

MD [m]	Gas ratio [-]	ROP [m/hr]	Normalized Gas ratio	Normalized ROP
3080	0.633	10.86	0.012171534	0.33272925
3081	3.297	13	0.075010615	0.410293585
3082	6.324	15.39	0.146412228	0.496919174
3083	9.728	12.62	0.226706609	0.396520478
3084	15.041	12.64	0.352030948	0.397245379
3085	20.039	11.97	0.469924989	0.372961218
3086	24.079	9.49	0.565221494	0.283073577
3087	24.201	8.97	0.568099259	0.264226169
3088	11.491	5.87	0.268292683	0.151866618
3089	6.474	15.76	0.149950465	0.51032983
3090	7.619	20.35	0.176959004	0.676694455
3091	7.591	28.47	0.176298533	0.971003987
3092	7.38	25.51	0.171321413	0.863718739
3093	9.784	27.54	0.228027551	0.937296122

Model Fitting and Analysis

Following the normalization and outlier removal, several models, such as linear, second-degree polynomial, power, and exponential, were applied to the data using MATLAB. The models were evaluated based on their R^2 value (which measures the fit goodness) and the sum squared error (SSE). In addition, the model that best suited the data was determined to have the highest R^2 value and the lowest SSE. This process was repeated for each of the three laterals to determine the most accurate model for each case.

For a more accurate and better analysis of the data, we used the graphs of MD in terms of gas ratio and ROP. We then proceeded to analyze the trends observed in these graphs for each lateral, as illustrated in Fig. 8 to Fig. 10 (The trends indicated in these figures should be observed and verified for each lateral in both MD vs. Gas ratio and MD vs. ROP graphs).

For better interpretation, the average data was calculated and plotted every 10 meters (The unclear parts in the graphs have been removed as they are outside the production zone according to their geosteering). Other methods, such as smoothing techniques, will also show the same trends.

Results

First, we plotted the normalized ROP vs. normalized gas ratio. Subsequently, different models were examined to determine the most suitable match for each lateral data set. For lateral 1, the second-degree polynomial model offered the most accurate correlation between ROP and gas ratio, with an R^2 value of 0.095 and an SSE of 12.77 (Table 3 and Fig. 11). In lateral 2, the second-degree polynomial model again provided the best fit, with an R^2 value of 0.344 and an SSE of 5.76 (Table 4 and Fig. 12). However, in lateral 3, the power model proved to be the most accurate, with an R^2 value of 0.207 and an SSE of 4.34 (Table 5 and Fig. 13). As it is clear from the results, the lateral 2 correlations have higher accuracy than the other two laterals (All equations are dimensionless).

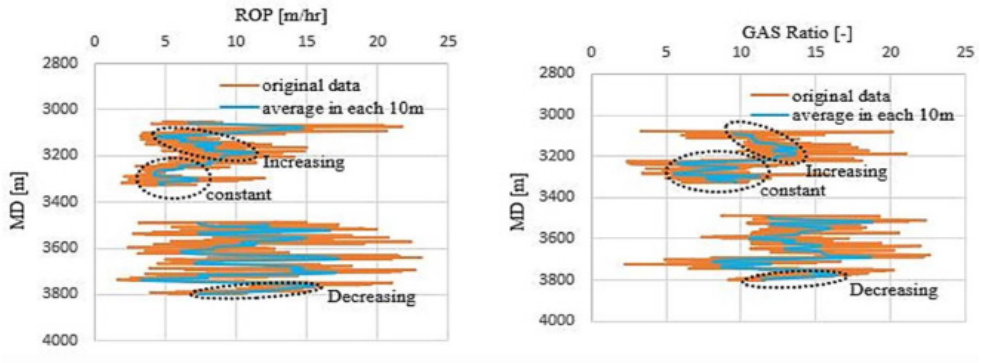

Fig. 8 Graphs of measurement depth (MD) in terms of ROP and Gas ratio for lateral 1.

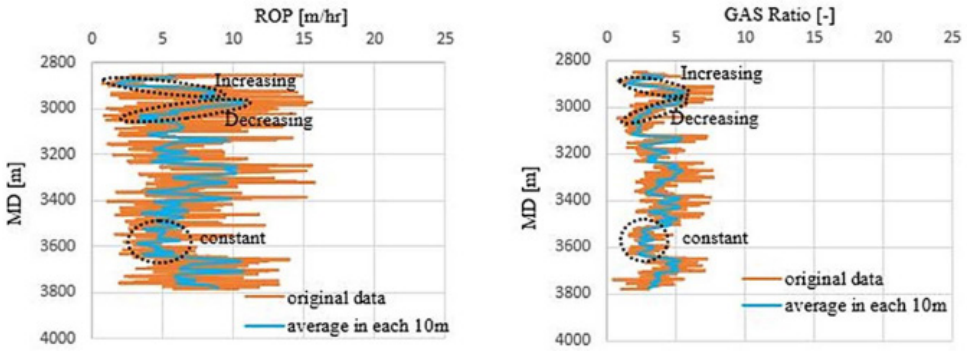

Fig. 9 Graphs of measurement depth (MD) in terms of ROP and Gas ratio for lateral 2.

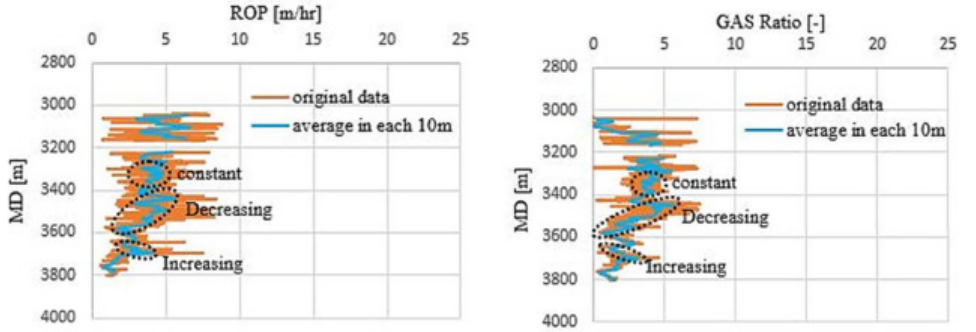

Fig. 10 Graphs of measurement depth (MD) in terms of ROP and Gas ratio for lateral 3.

Table 3 Accuracy and error of correlations - lateral 1.

Fit name	Data	Best fit type	SSE	R^2
Lateral 1 (total data)	ROP vs. Gas ratio	Linear	13.01	0.078
Lateral 1 (total data)	ROP vs. Gas ratio	Second degree-polynomial	12.77	0.095
Lateral 1 (total data)	ROP vs. Gas ratio	Power	12.79	0.094
Lateral 1 (total data)	ROP vs. Gas ratio	Exponential	12.9	0.086

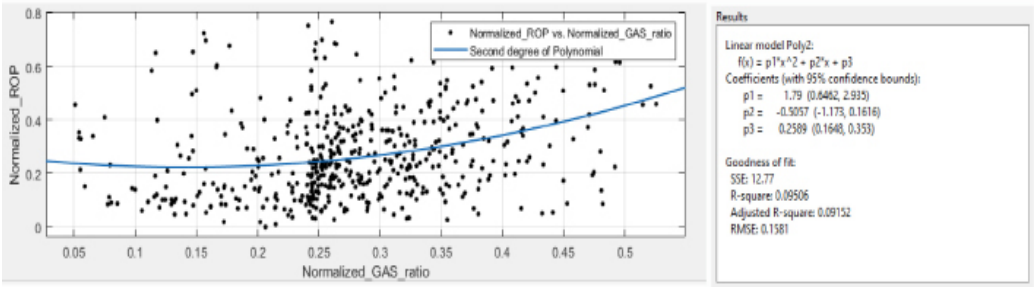

Fig. 11 Graph and equation of second degree-polynomial model for lateral 1.

Table 4 Accuracy and error of correlations - lateral 2.

Fit name	Data	Best fit type	SSE	R^2
Lateral 2 (total data)	ROP vs. Gas ratio	Linear	5.79	0.341
Lateral 2 (total data)	ROP vs. Gas ratio	Second degree-polynomial	5.76	0.344
Lateral 2 (total data)	ROP vs. Gas ratio	Power	5.77	0.343
Lateral 2 (total data)	ROP vs. Gas ratio	Exponential	6.01	0.316

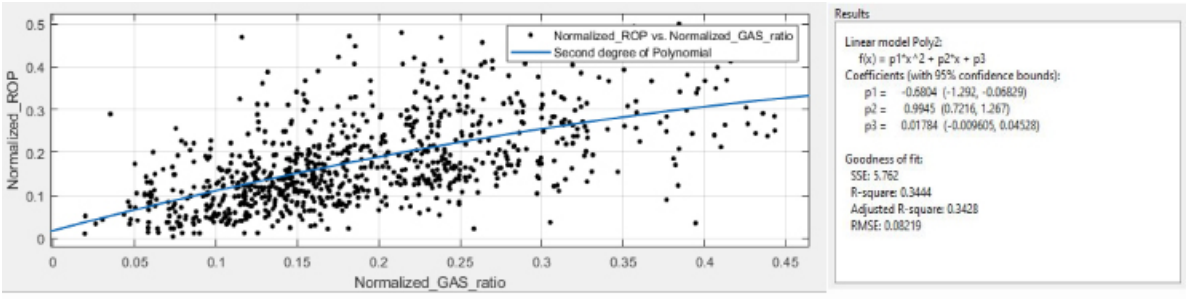

Fig. 12 Graph and equation of second degree-polynomial model for lateral 2.

Table 5 Accuracy and error of correlations - lateral 3.

Fit name	Data	Best fit type	SSE	R^2
Lateral 3 (total data)	ROP vs. Gas ratio	Linear	4.45	0.187
Lateral 3 (total data)	ROP vs. Gas ratio	Second degree-polynomial	4.36	0.204
Lateral 3 (total data)	ROP vs. Gas ratio	Power	4.34	0.207
Lateral 3 (total data)	ROP vs. Gas ratio	Exponential	4.39	0.197

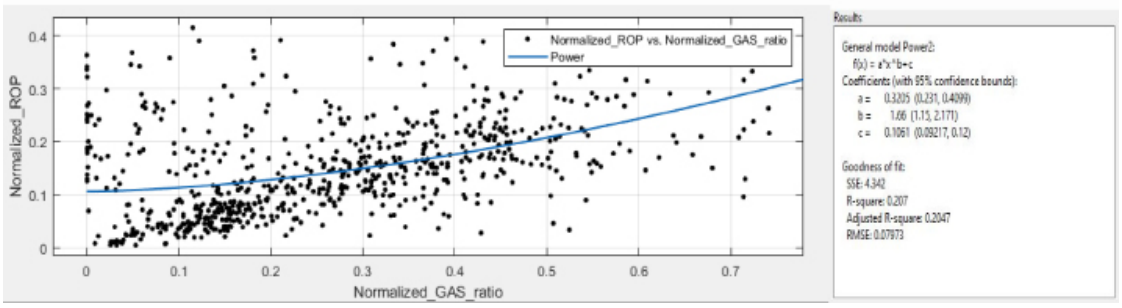

Fig. 13 Graph and equation of power model for lateral 3.

According to the MATLAB output, the equation of the best fit for lateral 1 is:

$$f(x)=1.79*x^2-0.5057*x+0.2589 \quad (4)$$

The best correlation equation for lateral 2 is:

$$f(x)=-0.6804*x^2+0.9945*x+0.01784 \quad (5)$$

The best correlation equation of lateral 3 is:

$$f(x)=0.3205*x^{1.66}+0.1061 \quad (6)$$

Because the correlations from the analysis of the total data were not sufficiently accurate, we analyzed the data based on different sections of MD graphs (according to Fig. 7 to Fig. 9), including the increasing, constant, and decreasing sections. For example, when we examine the increasing section, it indicates that in one part of the layer, both ROP and gas ratio parameters are increasing. It is likely that we have entered the reservoir layer because the drilling rate in the producing layer has increased due to the presence of porosity and fluid. Furthermore, the existence of hydrocarbons enhances the measured gas ratio. The analysis showed that the decreasing sections provided more accurate correlations for laterals 1 (Table 6 and Fig. 14) and 2 (Table 7 and Fig. 15), while the increasing section offered better accuracy for lateral 3 (Table 8 and Fig. 16). In addition, this variation is likely due to the heterogeneous nature of the reservoir, which introduces variability in the correlation between ROP and gas ratio.

Table 6 Accuracy and error of best correlations for increasing, constant, and decreasing sections - lateral 1.

Fit name	Data	Best fit type	SSE	R^2
Lateral 1 (increasing section)	ROP vs. Gas ratio	Second degree-polynomial	3.566	0.0153
Lateral 1 (constant section)	ROP vs. Gas ratio	Power	1.515	0.015
Lateral 1 (decreasing section)	ROP vs. Gas ratio	Second degree-polynomial	0.821	0.582

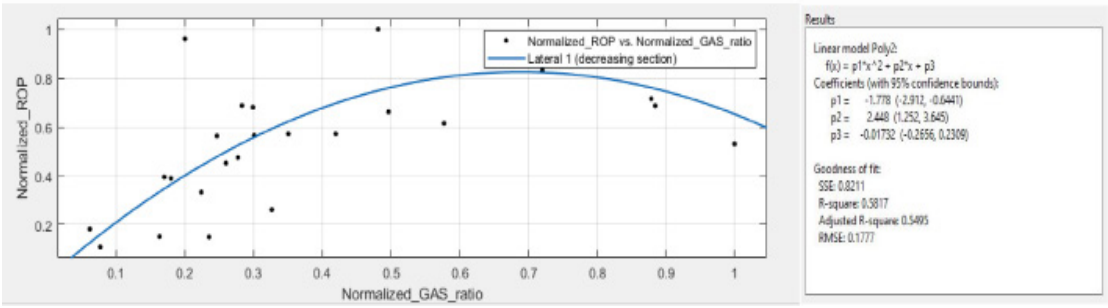

Fig. 14 Graph and equation of second degree-polynomial model (decreasing section) for lateral 1.

Table 7 Accuracy and error of best correlations for increasing, constant, and decreasing sections - lateral 2.

Fit name	Data	Best fit type	SSE	R^2
Lateral 2 (increasing section)	ROP vs. Gas ratio	Power	0.961	0.46
Lateral 2 (constant section)	ROP vs. Gas ratio	Power	1.353	0.08
Lateral 2 (decreasing section)	ROP vs. Gas ratio	Second degree-polynomial	0.389	0.657

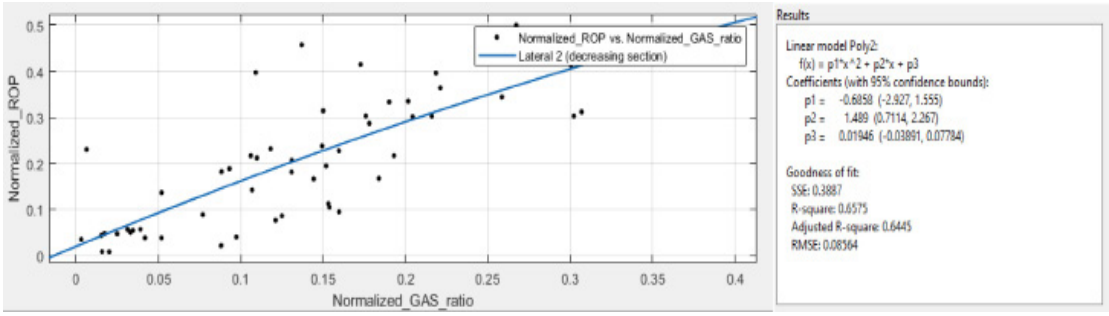

Fig. 15 Graph and equation of second degree-polynomial model (decreasing section) for lateral 2.

Table 8 Accuracy and error of best correlations for increasing, constant, and decreasing sections of lateral 3.

Fit name	Data	Best fit type	SSE	R^2
Lateral 3 (increasing section)	ROP vs. Gas ratio	Second degree-polynomial	0.495	0.554
Lateral 3 (constant section)	ROP vs. Gas ratio	Second degree-polynomial	2.14	0.235
Lateral 3 (decreasing section)	ROP vs. Gas ratio	Power	1.91	0.212

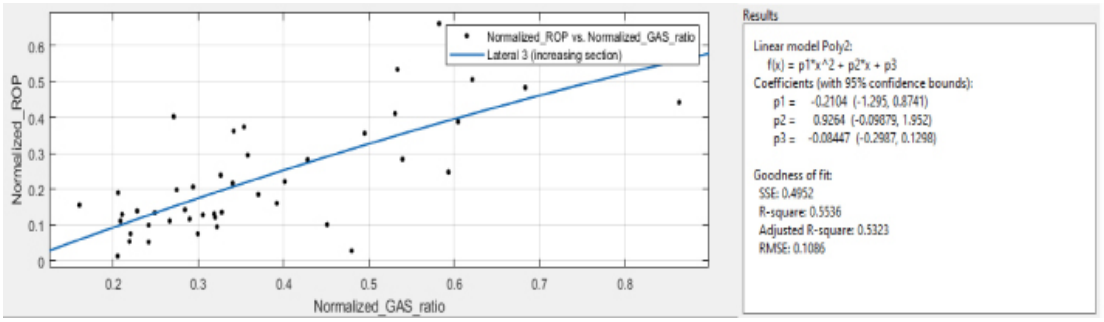

Fig. 16 Graph and equation of second degree-polynomial model (increasing section) for lateral 3.

The best correlation equation for decreasing section of lateral 1:

$$f(x)=-1.778*x^2+2.448*x-0.01732 \quad (7)$$

The best correlation equation for decreasing section of lateral 2:

$$f(x)=-0.6858*x^2+1.489*x+0.01946 \quad (8)$$

According to the MATLAB output, the equation of the best fit for increasing section of lateral 3 is:

$$f(x)=-0.2104*x^2+0.9264*x-0.08447 \quad (9)$$

Application

Heterogeneity indicates the variation in the values of various parameters of a reservoir, such as porosity and permeability, at different points within it, which ultimately causes changes in ROP and gas ratio. These three laterals were drilled at different locations in the reservoir, and the variations in the fitting results demonstrate the presence of heterogeneity in the reservoir. This paper opens a new window for studying the correlation between two or more drilling parameters for reservoir identification. Using this method, it is possible to better understand the geomechanical properties of the rock and optimize drilling parameters, including RPM, ROP, WOB, etc. It further helps reduce expenses that result from improper drilling.

Discussion

These laterals are located in a heterogeneous reservoir, and the data used in this study are real. Therefore, the different results for each lateral can be justified to some extent. This study mainly deals with the existence or absence of a correlation between ROP and gas ratio in the reservoir layer. As long as this correlation is established in the reservoir, we can drill in the appropriate direction without having to use geosteering again. Using all geomechanical data of the rock and well logging, which provide a better understanding of the reservoir, is essential when applying these correlations. For each reservoir, a specific correlation is established based on its properties. Different correlations can be seen in reservoirs of limestone, shale, and sandstone. Future work should explore applying these models to other fields with similar geological characteristics to validate their broader applicability (The procedure is shown in a flowchart in Fig. 17). Additionally, integrating more advanced machine learning algorithms may further enhance the accuracy of the correlations and reduce the need for manual intervention during the drilling process.

Fig. 17 Procedure Flowchart

Conclusion

An important aspect of geosteering involves steering wells in horizontal layers, usually achieved by correlating the gamma-ray logs from a lateral with the logs from a vertical reference well. Many technologies, such as machine learning and automatic geosteering, have been developed in this field; however, they often incur significant costs due to the frequent use of geosteering.

This study explored the correlation between ROP and gas ratio data for three laterals drilled in a heterogeneous limestone reservoir in Iran by plotting normalized ROP vs. normalized gas ratio. By fitting various mathematical models to the normalized data, we identified (for total data analysis) the second-degree polynomial model as the most accurate for laterals 1 and 2. In contrast, the power model provided the best fit for lateral 3. The research revealed that the second-degree polynomial model was the most accurate for the three laterals based on data from various parts of MD graphs. These correlations offer a valuable tool for optimizing future drilling operations in the field, potentially reducing the need for repeated geosteering and the associated costs.

Nomenclature

$gas\ ratio_{norm}$: Normalized gas ratio
IGR : Interquartile Range
LWD: Logging While Drilling
MD: Measurement Depth, m
MWD: Measurement While Drilling

R^2: Fit Goodness
RMSE: Root Mean Squared Error
ROP: Rate Of Penetration, m/hr
ROP_{norm}: Normalized Rate Of Penetration
Sar: Sarvak Layer
SSE: Sum Squared Error
TST: True Stratigraphic Thickness, m
TVD: True Vertical Depth, m
WOB: Weight On Bit, kIb

References

1. Rogii. (2018), Starsteer Manual, The most efficient and easy to use Geoscience Software, StarSteer empowers Geologists and Geoscientists to steer wells in real-time, visualize well logs, map subsurface geology, and plan well trajectories for optimal well placement and reservoir performance, RGOI Technology, Houston, Texas, The USA.
2. Nascimento, A. (2012). Drilling Fluid: A stochastic ROP optimization approach for the Brazilian pre-salt carbonates, Leoben, Montan University.
3. Othmer, K. (2002). Encyclopedia of Chemical Technology, Fourth Editon, Published by Pergamon Press Ltd. (This is a translation of the eleventh edition of the German work Grundriß der Chemischen Technik published by Verlag Chemie, GmbH, Weinheim), Headington Hill Hall, Oxford, The UK, 13, 1-847.
4. Dashti, J., Al-Awadi, M., Al-Ajmi., B., & Rao, S. (2016). Use of advanced mud gas chromatography for reservoir quality prediction while drilling, IPTC, 18624, doi. org/10.2523/IPTC-18624-MS.
5. Al-Maskeen, A., Sung, R., & Ali, S. (2013). Horizontal well correlation using real time data and log prediction in geosteering complex reservoirs of Saudi Arabia, In SPE Middle East Oil and Gas Show and Conference, 164151, doi.org/10.2118/164151-MS.
6. Maus, S., Gee, T., M. Mitkus, A., McCarthy, K., Charney, E., Ferro, A., Liu, Q., Lightfoot, J., Reynerson, P., & Velozzi, D. (2020). Automated geosteering with fault detection and multi-solution tracking, SPE, IADC, 199660, doi.org/10.2118/199660-MS.
7. Heintzelman, L., Willerth, M., Elhaj, N., & Eaton, J. (2022). Field validation of an automated geosteering algorithm in the haynesville shale, IADC/SPE, 208697, doi.org/10.2118/208697-MS.
8. Angelo, J., Zhao, Z., Zhang, Y., Ashok, P., Chen, D., & Oort, E. (2024). Real-time automated geosteering interpretation combining log interpretation and 3D Horizon Tracking, Geosciences, 14030071, doi. org/10.3390/geosciences14030071.
9. Alyaev, S., Suter, E., Brumer Bratvold, R., Hong, A., Luo, H., & Fossum, K. (2019). A decision support system for multi-target geosteering, Elsevier, 183, 106381, doi. org/10.1016/j.petrol.2019.106381.
10. Fjellheim, R., Herbert, M., Arild, O., Bisio, R., & Holo, O. (2010). Collaboration and Decision Support in Geosteering, SPE, 128721, dx.doi.org/10.2523/128721-MS.
11. Rajaieyamchee, M. A., & Bratvold, R. B. (2010). A decision analytic framework for autonomous geosteering. In SPE Annual Technical Conference and Exhibition? (pp. SPE-135416). SPE., doi.org/10.2118/135416-MS.
12. Shen, Q., Wu, X., Chen, J., Han, Z., & Huang, Y. (2017). Solving geosteering inverse problems by stochastic hybrid monte carlo method, Petroleum Science and Engineering, 161, doi.org/10.1016/j.petrol.2017.11.031, 9-16.
13. Winkler, H. (2017). Geosteering by exact inference on a Bayesian network, Geophysics, 0569, dx.doi. org/10.1190/geo2016-0569.1
14. Bittar, M., Klein, J., Beste, R., Hu, G., Wu, M., Pitcher, J., Golla, C., Althoff, G., Sitka, M., Minosyan, V., & Paulk, M., (2009). A new azimuthal deep-reading resistivity tool for geosteering and advanced formation evaluation. SPE Reservoir Evaluation & Engineering, 12(02), 270-279, doi.org/10.2118/109971-PA, 270-279.
15. Tilsley-Baker, R., Antonov, Y., Martakov, S., Maurer, H., Mosin, A., Sviridov, M., Sandler Klein, K., Iversen, M. (2013). Eustaquio Barbosa. J and Carneiro. G, Extra-Deep Resistivity Experience in Brazil Geosteering Operations, SPE, 166309, doi.org/10.2118/166309-MS
16. Mottahedeh, R. (2008). Horizontal well geosteering: planning, monitoring and geosteering, Canadian Petroleum Technology, doi.org/10.2118/08-11-28-CS
17. Thevoux-Chabuel, H., & Fejerskov, M., (2006). Geosteering diagnosis: a new approach to monitor the well position within a 3D geological model, In SPE Annual Technical Conference and Exhibition?, 102602, doi.org/10.2118/102602-MS.
18. Zongguo, W., Xing, L., Jianyi, D., Zhaofeng, L., Zhao, Z., Gaocheng, W., Yang, G., & Xun, L. (2017). Application of 3D geosteering in geology-engineering integration practice, China Petroleum Exploration, 22, 1, doi.org/10.3969/j.issn.1672-7703.2017.01.011.
19. Wang. S, Yuan. S, Wang. T, Gao. J and Li. S. (2018). Three-dimensional geosteering coherence attributes for deep-formation discontinuity detection, Geophysics, doi.org/10.1190/geo2017-0642.1.
20. Vladimirovich Denisenko. I, Andreevich Kuvaev. I, Borisovich Uvarov. I, Evgenievich Kushmantzev. O and Igorevich Toporov. A. (2020). Automated Geosteering While Drilling Using Machine Learning. Case Studies, In SPE Russian Petroleum Technology Conference (p. D023S009R004). doi.org/10.2118/202046-MS.
21. Gupta, I., Tran, N., Devegowda, D., Jayaram, V., Rai, C., Sondergeld, C., & Karami, H. (2020). Looking ahead of the bit using surface drilling and petrophysical data: Machine-learning-based real-time geosteering in volve field. SPE Journal, 25(02), 990-1006. Gupta, I., Tran, N., Devegowda, D., Jayaram, V., Rai, C., Sondergeld, C., & Karami, H. (2020). Looking ahead of the bit using surface drilling and petrophysical data: Machine-learning-based real-time geosteering in volve field. SPE Journal, 25(02), 990-1006.
22. Galkina, A. V., Yalaev, T. R., Lisitsyna, M. Y., & Rakhimov, T. R. (2020). Geosteering based on integration of LWD and surface logging using machine learning. In SPE Russian Petroleum Technology Conference (p. D043S032R006). doi.org/10.2118/201945-MS.